Electrochemically Grafted Gallic Acid-Chitosan: A metal-free *in situ* redox platform for regiospecific oligopeptide-viral spike protein interaction

Vinoth Krishnan[a,b], Chinnaiah Sivakumar[a,b], Kannadasan Anand Babu[c], Sevakumaran Vigneswari[d], Rajamani Lakshminarayanan[e], Sudhakar Natarajan[f], Murugan Veerapandian[a,b*]

[a]*Electrodics and Electrocatalysis Division, CSIR-Central Electrochemical Research Institute (CECRI), Karaikudi, 630 003, Tamil Nadu, India.*

[b]*Academy of Scientific & Innovative Research (AcSIR), Ghaziabad-201 002, India.*

[c]*Anderson Clinical Genetics, Anderson Diagnostics and Labs, Chennai, Tamil Nadu, India.*

[d]*Institute of Climate Adaptation and Marine Biotechnology (ICAMB), Kuala Nerus 21030, Terengganu, Malaysia.*

[e]*Ocular Infections and Antimicrobials Research Group, Singapore Eye Research Institute, The Academia, 20 College Road, Discovery Tower, Singapore 169856, Singapore.*

[f]*Department of Virology and Biotechnology, ICMR-National Institute for Research in Tuberculosis (NIRT), Chennai 600031, Tamil Nadu, India.*

*Corresponding Author

Email: vmurugan@cecri.res.in (M. Veerapandian); Tel: +91-4565 241384

Materials and Instrumentation

Chitosan (low molecular weight 50,000–190,000 g mol^{-1}, viscosity 20–300 cp, 75–85% deacetylated) and Gallic acid are purchased from Sigma Aldrich. Mix&Go™ Biosensor and Tris-EDTA buffer solution were procured from Sigma-Aldrich. All other chemicals and solvent were of research grade and used without further purification. Deionized (DI) water from Millipore system with resistivity >18.2 MΩ/cm was used throughout the experimental condition. A carbon-based screen-printed electrode (SPE) from Zensor R&D, containing an integrated carbon as working (2 mm diameter) and counter electrode (C-shaped), with the circular shaped Ag/AgCl as reference electrode was used as base for sensor. All the experiments were performed in triplicate. From the identified conserved Fab region of SARS-CoV-2 neutralizing antibodies the target specific probe oligopeptides and negative control oligopeptide has been designed for biosensor fabrication. As custom designed sequence was synthesized commercially by Priveel Peptides, India.

Probe peptide: RGEMTAVFGDYWGQG
Negative peptide: FGHIKLMNPFGAACNPQRSTVWWYACDEFGDEFGHIKYAACDE

Surface chemistry of EgGC electrode was studied using X-ray photoelectron spectroscopy (XPS), an ESCALAB 250XI BASE system with Al Kα as a probe. The high-resolution C 1s, O 1s and N 1s spectra were fitted using CASA XPS software. The surface morphology of EgGC was characterized by field-emission scanning electron microscopy (FESEM), Carl Zeiss, Germany (model: SUPRA 55VP), Gemini column, with an air-lock system. Electrochemical studies were carried out using an OrigaLys, Model: OGF500. Real sample validation was done using the portable Rodeostat instrument.

Experimental Procedure

Chitosan (10 mg/mL) was electrodeposited using galvanostatic method at an applied potential of −1.5 V for 15 min on the cathode (pristine CSPE) and dried. Afterward, the fabricated CS/SPE surface was underwent for the electrochemical grafting of GA using potentiodynamic technique, cyclic voltammetry (CV). A potential sweep in the range of −0.2 to +0.9 V at a scan speed of 0.05 V/s for 25 cycles in an optimal acidic electrolyte condition H_2SO_4 (0.05 M) with 0.01 M of GA was used to achieve the grafting of gallic acid-chitosan (EgGC) matrix.

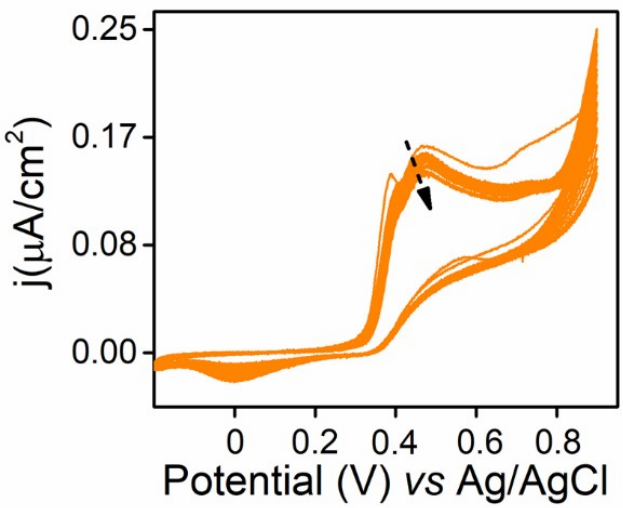

Fig. S1 CV measurement for the electrochemical grafting of gallic acid on chitosan (EgGC) deposited screen printed electrode.

Electrokinetic Parameters

The electrochemical surface area of EgGC was calculated using Randles−Sevcik equation as follows

$$I = 2.69 \times 10^5 n^{3/2} A D^{1/2} C v^{1/2}$$

where I is the peak current (A), n is the number of electrons involved in the redox reaction, A is the electrochemical area (cm^2), D is the diffusion coefficient of the redox probe (6.7 ×10−6 cm^2/s), C is the concentration of the redox probe (5 mM of $K_3[Fe(CN)_6]/K_4[Fe(CN)_6]$) in a supporting electrolyte of 0.1 M KCl, and v is the scan rate (0.05 V/s) used in the experiment.[1]

The impedance spectra from the experiments were analyzed using ZSimpWin3.6 software, which enabled the fitting of experimental data to simulated data for comparison. The quality of the fit was evaluated using the chi-square value, which measures the difference between experimental and simulated data. A lower chi-square value indicates a better fit between the two. In this study, a chi-square value around 10^{-3} was considered to represent an excellent fit with a minimal number of components, indicating that the simulated data closely matched the experimental results, providing accurate and reliable insights into the system's impedance behavior.

The electric double layer capacitance is obtained from the capacitance tool of inbuilt Origamaster software in Origalys electrochemical workstation (model: OGF^+ 500), by viewing the measured electrochemical impedance spectra.

CV response of prepared EgGC electrode at different scan rate (0.01 to 0.09 V/s) in 0.1M PBS (pH 7.4) as an electrolyte. As observed current density was linearly increased (0.25 to 0.48 μA/cm^2) with respect to scan rate from 0.01 to 0.09 V/s, indicating a coefficient of determination (R^2) value of 0.98. From the derivative plot of scan rate *vs* peak current, it is confirmed that the surface confined process is occurred at the electrode-electrolyte interface.

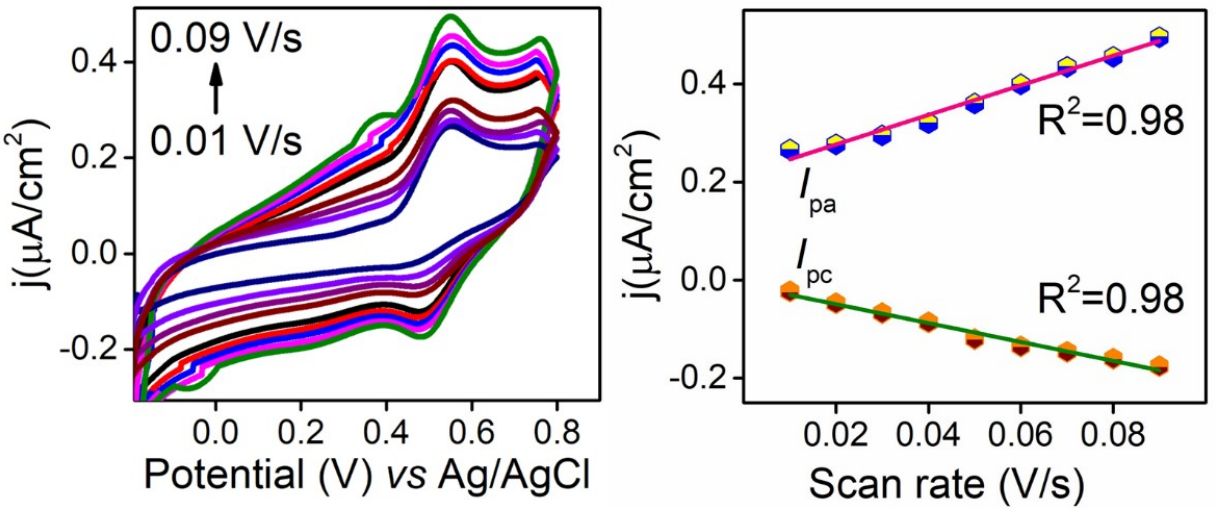

Fig. S2 Scan rate dependence study of EgGC electrode platform and its linear plot.

Electrochemical redox mechanism of EgGC platform

As developed EgGC electrode platform exerts a reversible redox behaviour, which is due to the conversion of catecholic OH group to quinone moiety at an anodic peak potential of +0.55 V. This electrochemical conversion follows two electron two proton ($2e^-$ $2H^+$) at the electrode-electrolyte interface.

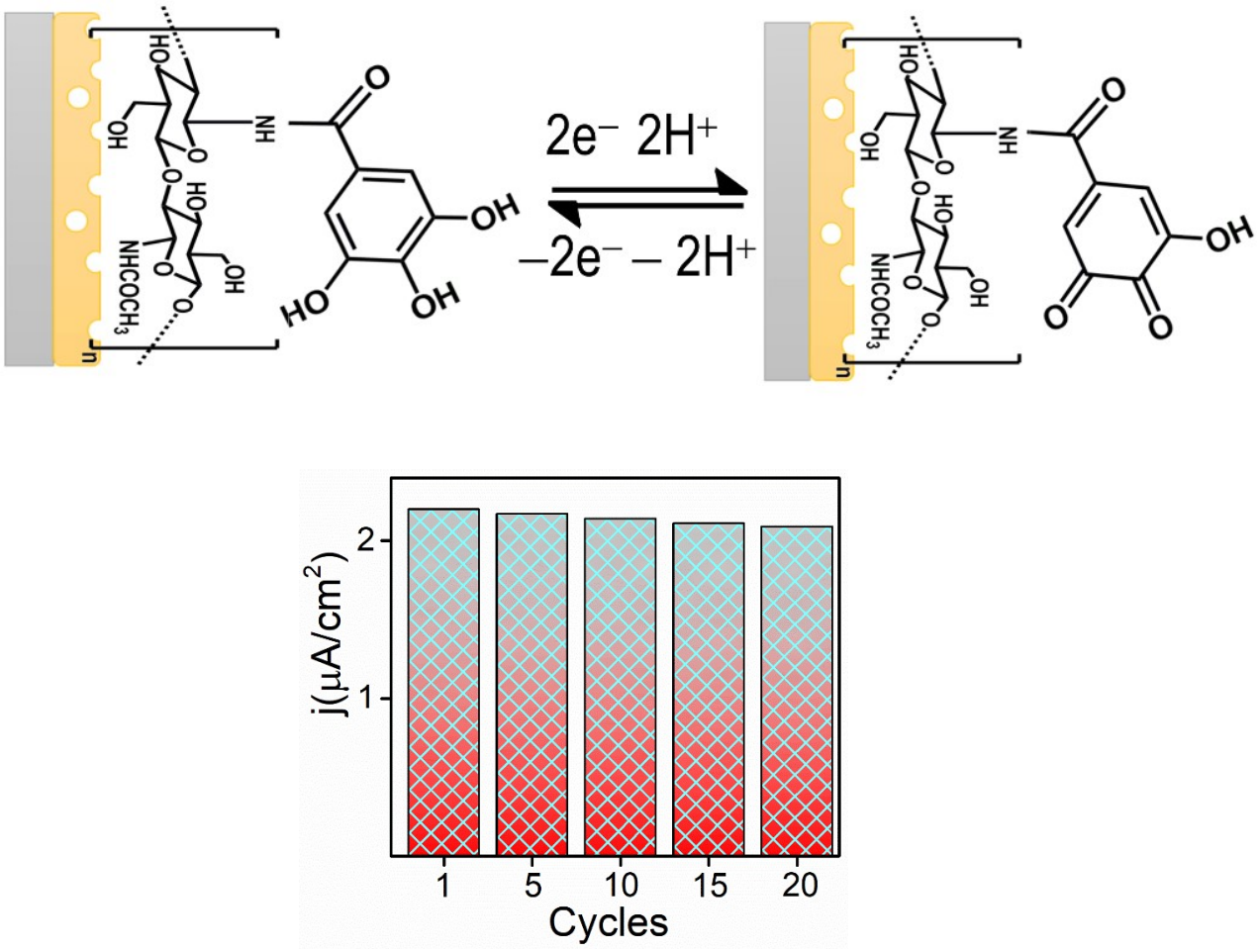

Fig. S3 Electron transfer mechanism of EgGC electrode platform and histogram derived from the CV analysis of the developed EgGC electrode for 20 cycles in PBS (pH 7.4) electrolyte medium

Field Emission-Scanning Electron Microscopy Analysis

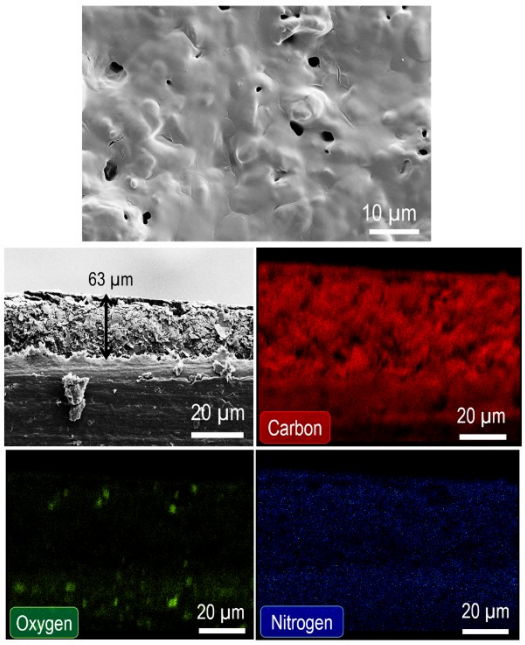

Fig. S4 Surface topography, cross-sectional image, and its elemental mapping of EgGC on the SPE platform.

X-ray Photoelectron Spectroscopy (XPS)

XPS survey of EgGC clearly enabling the elemental presence of C1s, O1s and N1s centered at the binding energy of 283 eV, 532 eV and 400 eV, respectively.

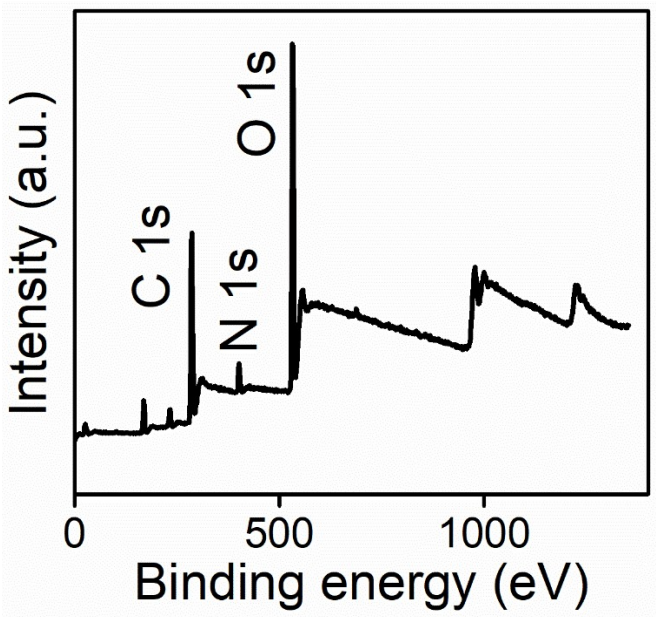

Fig. S5 XPS survey spectra of EgGC electrode platform.

XPS depth profile of EgGC

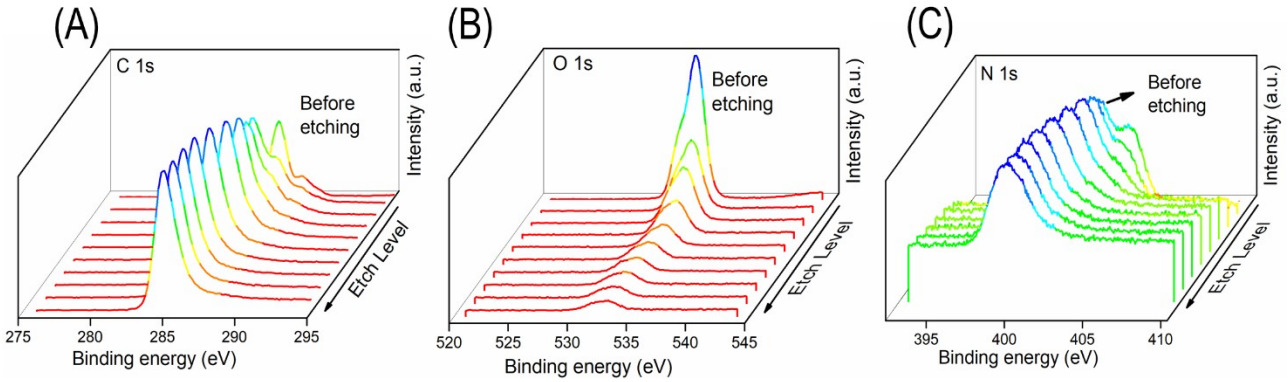

Fig. S6 High-resolution XPS analysis. Depth profiling of (A) C1s (B) O1s (C) N1s from EgGC electrode platform.

XPS plot of CS/SPE shows the C1s spectrum is fitted into three components associated to C–C, C-OH and C–N observed at 283.39, 284.89 and 286.52 eV, respectively. While the O1s peak shows two resolved peaks centered at 529.77 and 531.56 eV attributed to C=O and C-OH, respectively. The N1s spectra exhibits two characteristic peaks associated to C-N (398.9 eV) and N-H (401 eV) of glucosamine ring in CS.

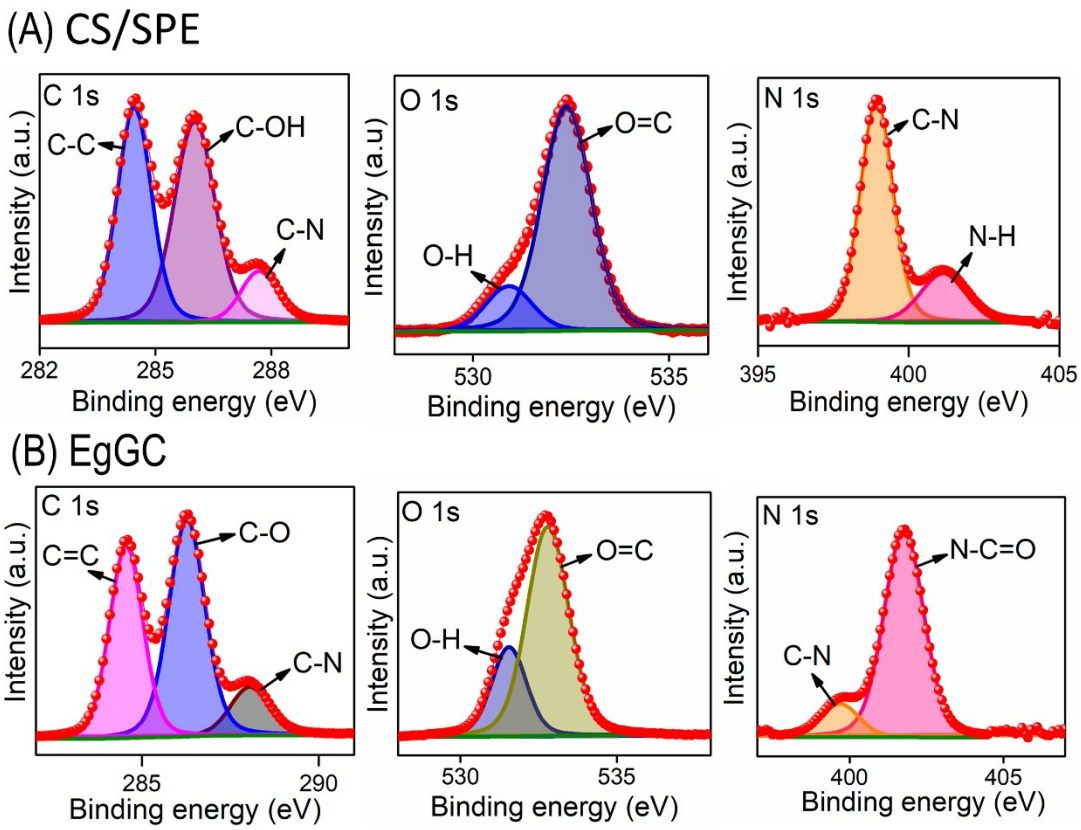

Fig. S7 High resolution XPS spectra of C 1s, O 1s, and N 1s of CS-SPE (A) and EgGC (B).

Electrochemical Peptide Biosensor Platform Construction

To fabricate an electrochemical biosensor platform for point-of-care usage, as prepared EgGC electrode platform was modified with bioaffinity layer (5 µL, 1 µg/mL) and allow it to dry for 10 minutes. Afterward probe oligopeptide sequence (5 µL, 100 nM) was immobilized on the activated surface and dried for 15 minutes. To avoid the non-specific interaction and to cover the void spaces, BSA (3 µL, 1 µg/mL) was utilized as the blocking agent (BSA-PP/b-EgGC) on the electrode matrix. Target spike protein (5 µL) was added to the biosensor platform and incubated for 15 min. Prepared sensor platforms were subjected for washing by immersing in PBS solution (pH 7.4) for 5 s, after modification with bioreceptor (oligopeptides) and target samples. All the experiments were performed using the 0.1 M PBS (pH 7.4) as the supporting electrolyte.

This label-free electrochemical biosensor typically consists of a redox probe on the electrode surface, with biosensor elements anchored or immobilized on top. In this case, the EgGC acts as the redox probe, and a bioaffinity layer is introduced over the electrode for the soft immobilization of the peptide, followed by bovine serum albumin (BSA) to cover unbound sites (BSA-Pep/b-EgGC). This sensor platform specifically targets the spike protein, and the corresponding electrochemical signal is monitored for detection.

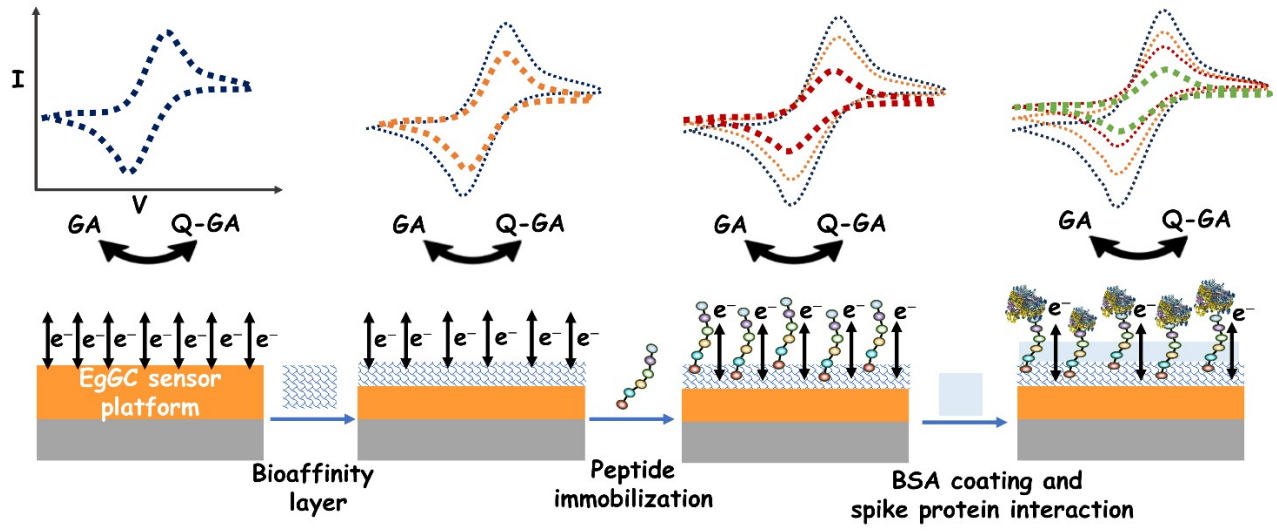

Fig. S8 Illustration on electrochemical biosensor layers and its associated pictorial cyclic voltammograms depicting the selective quenching of redox signal attributed to the conversion of C4/C5-OH of GA to quinone groups.

Regiospecific Oligopeptide Design and Synthesis

Human monoclonal antibody (002-S21F2) that targets the receptor-binding domain (RBD) of SARS-CoV-2 and effectively neutralizes the SARS-CoV-2 variants of concern (VOCs) such as Alpha, Beta, Gamma, Delta, and Omicron (BA.1 and BA.2).[2] The regiospecific oligopeptide sequence was designed from the complementarity-determining region of the variable domain of heavy chain (CDRH3) of the human monoclonal antibody (002-S21F2) for the detection of the SARS-CoV-2 VOCs through an electrochemical biosensor technique. The designed oligopeptide was validated by the *in-silico* methods for its binding capacity with the RBD of SARS-CoV-2 VOCs. The Tripos' SYBYL-X (version 1.3) was used to perform the *in-silico* assay.[3] Molecular docking results indicates that designed RG-15 oligopeptide exert a good interaction with the spike proteins of SARS-CoV-2, evidenced with a total Sybyl score >5 and consensus score (Cscore) of 5. It was found that more than 8 residues interact with high affinity and hydrogen bond of <3 Å. The quality of the synthesised oligopeptides were analyzed by mass spectrometry and HPLC (Fig. S8 and S9).

Note:

Peptide synthesis-002-S21F2

RGEMTAVFGDYWGQG

Cloning and Expression

>4A8 heavy chain

GAGATCGTGATGACCCAGAGCCCCCTGAGCAGCCCCGTGACCCTGGGCCAGCCCGCCAGC
ATCAGCTGCAGGAGCAGCCAGAGCCTGGTGCACAGCGACGGCAACACCTACCTGAGCTGG
CTGCAGCAGAGGCCCGGCCAGCCCCCCAGGCTGCTGATCTACAAGATCAGCAACAGGTTC
AGCGGCGTGCCCGACAGGTTCAGCGGCAGCGGCGCCGGCACCGACTTCACCCTGAAGATC
AGCAGGGTGGAGGCCGAGGACGTGGGCGTGTACTACTGCACCCAGGCCACCCAGTTCCCC
TACACCTTCGGCCAGGGCACCAAGGTGGACATCAAGAGGACCGTGGCCGCCCCCAGCGTG
TTCATCTTCCCCCCCAGCGACGAGCAGCTGAAGAGCGGCACCGCCAGCGTGGTGTGCCTG
CTGAACAACTTCTACCCCAGGGAGGCCAAGGTGCAGTGGAAGGTGGACAACGCCCTGCAG
AGCGGCAACAGCCAGGAGAGCGTGACCGAGCAGGACAGCAAGGACAGCACCTACAGCCTG
AGCAGCACCCTGACCCTGAGCAAGGCCGACTACGAGAAGCACAAGGTGTACGCCTGCGAG
GTGACCCACCAGGGCCTGAGCAGCCCCGTGACCAAGAGCTTCAACAGGGGCGAGTGC

>SARS2-38 Fab

CAGGTGCAGCTGAAGGAGAGCGGCCCCGGCCTGGTGGCCCCCAGCCAGAGCCTGAGCATC
ACCTGCACCGTGAGCGGCTTCAGCCTGACCAGGTACGGCGTGCACTGGGTGAGGCAGCCC
CCCGGCAAGGGCCTGGAGTGGCTGGGCGTGATCTGGGCCGACGGCAGCACCTACTACAAC
AGCGCCCTGATGAGCAGGCTGAGCATCAGCAAGGACAACAGCAAGAGCCAGGTGTTCCTG
AACATGAACAGCCTGCAGACCGACGACACCGCCAAGTACTACTGCGCCAGGGACGGCAGG
GGCTACGACGACTACTGGGGCCAGGGCACCACCCTGACCCAGATCGTGCTGACCCAGAGC
CCCGCCATCATGAGCGCCAGCCCCGGCGAGAAGGTGACCATGACCTGCAGCGCCAGCAGC
ACCGTGAGCTTCATCTACTGGTACCAGCAGAAGCCCGGCAGCAGCCCCAGGCTGCTGATC
TACGACACCAGCAACCCCGCCAGCGGCGTGCCCGTGAGGTTCAGCGGCAGCGGCTGCGGC
ACCAGCTACTACCTGACCATCAGCAGGATGGAGGCCGAGGACGCCGCCACCTACTACTGC
CAGCAGTGGAACACCTACCCCCTGACCTTCGGCGCCGGCACCAAGCTGGAGCTG

peptide synthesis- 002-S21F2

RGEMTAVFGDYWGQG

Raw Name	Total Score	Crash	Polar	D SCORE	PMF SCORE	G SCORE	CHEM SCORE	C SCORE	GLOBAL CSCORE
RG-15_1	5.4868	-1.3232	4.3845	-99.1185	16.5197	-132.411	-10.4618	5	5
RG-15_2	5.3836	-1.3915	0	-107.732	49.2176	-158.59	-19.4714	4	4
RG-15_3	5.3585	-1.0466	5.7818	-104.011	4.7872	-137.725	-9.517	2	3
RG-15_4	5.1852	-0.7098	0.9067	-87.9618	29.1106	-129.777	-16.7736	3	3
RG-15_5	4.6189	-1.0082	2.4973	-116.433	34.343	-118.972	-17.9771	4	3
RG-15_6	4.1613	-0.5588	2.9639	-87.0222	9.1375	-70.6478	-16.9084	5	3
RG-15_7	4.1566	-0.8475	0.0006	-100.729	18.6571	-147.43	-15.6313	4	3
RG-15_8	3.9714	-1.0413	4.2382	-90.1411	36.5593	-139.334	-13.3674	1	3
RG-15_9	3.8875	-2.4937	2.8078	-215.492	162.7008	-266.667	-20.7246	4	4
RG-15_10	3.8143	-1.7851	3.5903	-114.575	25.766	-161.33	-24.274	4	4
RG-15_11	3.5808	-1.5086	3.5322	-110.675	-10.1725	-171.825	-8.2242	4	4
RG-15_12	3.3947	-0.6106	1.7028	-88.1905	16.5716	-114.08	-15.7893	4	3
RG-15_13	3.3846	-0.5304	2.2368	-59.6998	33.1559	-127.036	-20.3805	4	3
RG-15_14	3.2988	-0.8243	2.1532	-70.0953	17.4326	-48.9152	-16.3421	2	3
RG-15_15	3.2263	-0.6505	1.0519	-54.9313	3.0796	-112.46	-12.9664	5	3
RG-15_16	3.1609	-0.198	0	-54.0877	3.1563	-125.168	-14.0072	5	3
RG-15_17	3.0406	-0.8479	0.0117	-108.328	-13.0433	-189.456	-13.3795	5	4
RG-15_18	2.8839	-0.6024	1.1784	-65.6711	7.1699	-94.4819	-10.1813	5	3
RG-15_19	2.8654	-1.1752	1.0769	-85.7439	34.901	-145.673	-12.1633	4	3
RG-15_20	2.8462	-0.4744	1.3684	-68.2707	21.6116	-96.0523	-13.4575	4	3

Molecular Docking Results

Table S1. RG-15_1 to 20 denotes different poses of docking results. Out the 20 docking poses we selected the best one and name it as RG-15_1.

Molecular docking study between oligopeptide and spike proteins of SARS-CoV-2

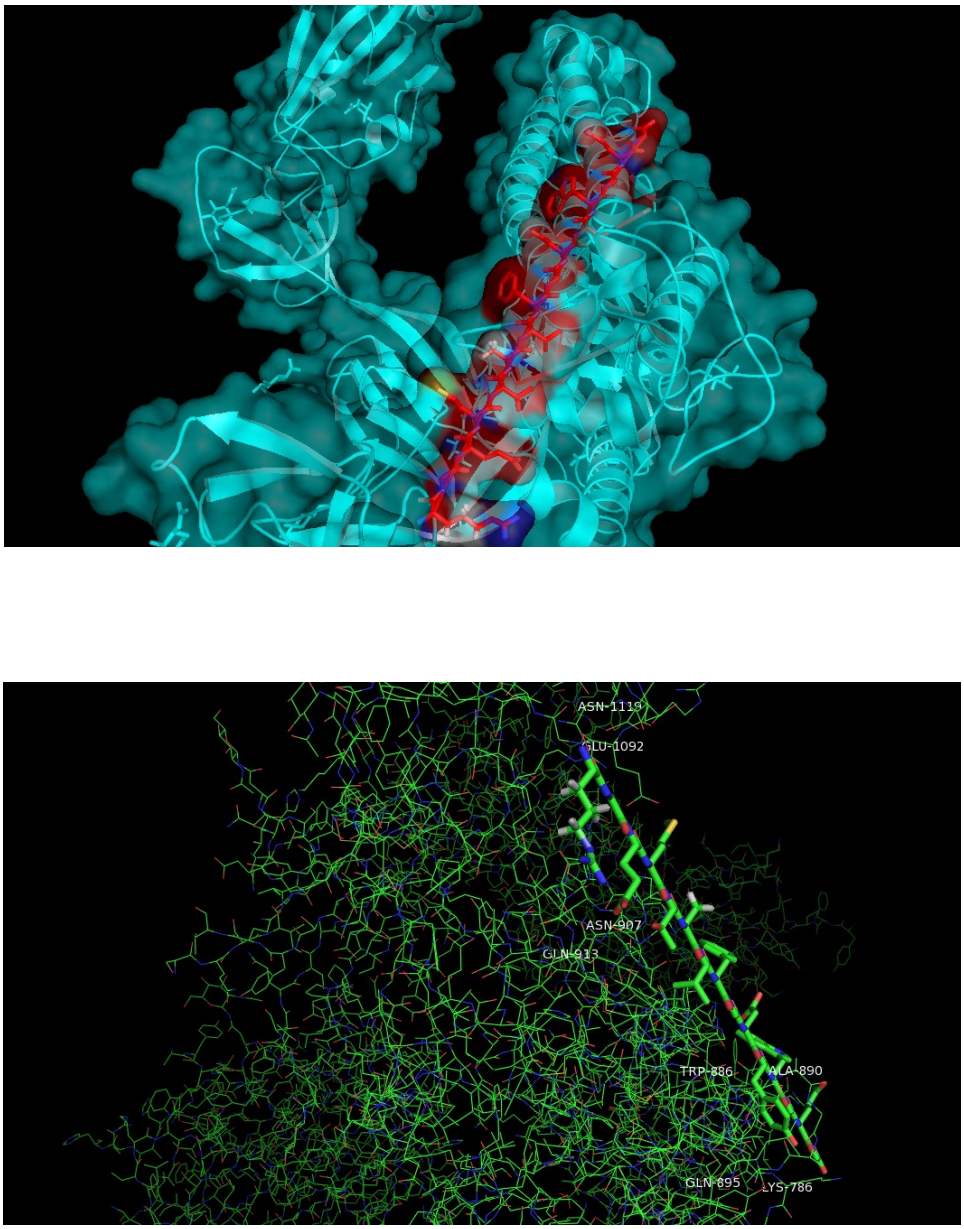

Fig. S9 Best docked poses of oligopeptide (RG-15) with spike protein.

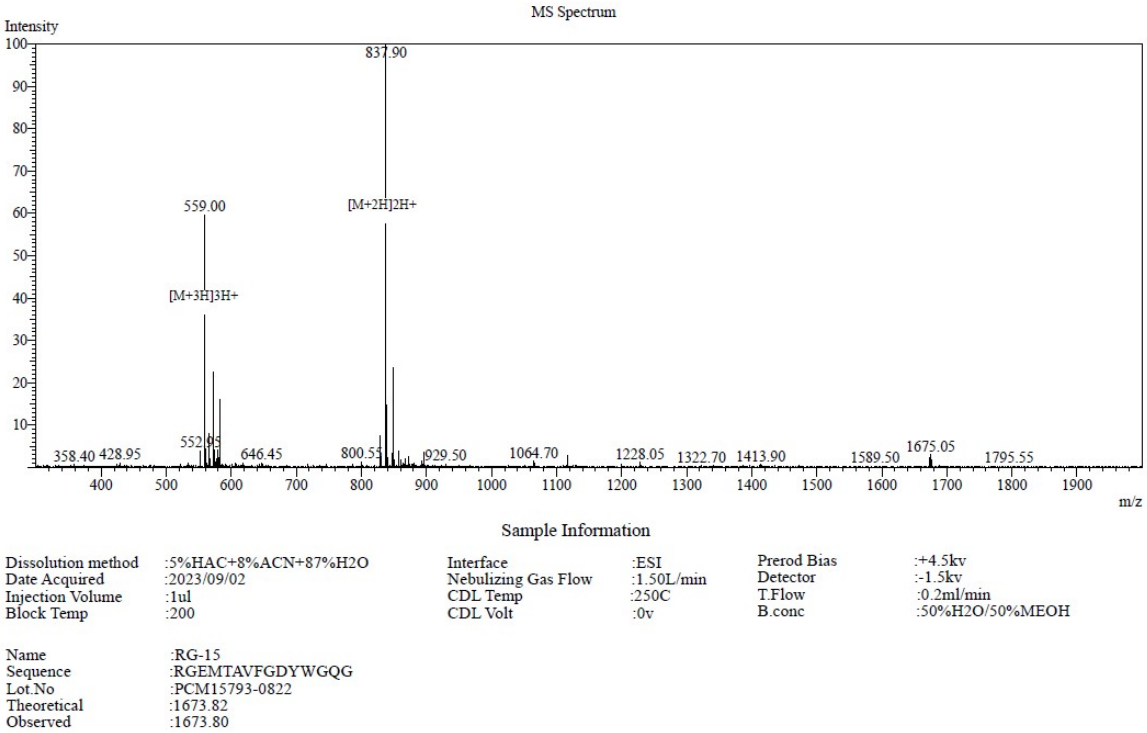

Fig. S10 Mass spectrum of the customized probe oligopeptide sequence.

HPLC Analysis

Name	:RG-15
Sequence	:RGEMTAVFGDYWGQG
Lot.No	:PCM15793-0822
Pump A	:0.1%Trifluoroacetic in 100% water
Pump B	:0.1%Trifluoroacetic in 100% acetonitrile
Total Flow	:1ml/min
Wavelength	:220nm
Analytical column type	:SHIMADZU Inertsil ODS-SP(4.6*250mm*5um)
Dissolution method	:15%ACN+85%H2O
Inj. Volume	:5 uL

Time	Module	Action	Value
0.01	Pumps	B.Conc	20
20.00	Pumps	B.Conc	60
23.00	Pumps	B.Conc	100
38.00	Pumps	B.Conc	100
40.00	Pumps	B.Conc	20
50.00	Controller	Stop	

Chromatogram

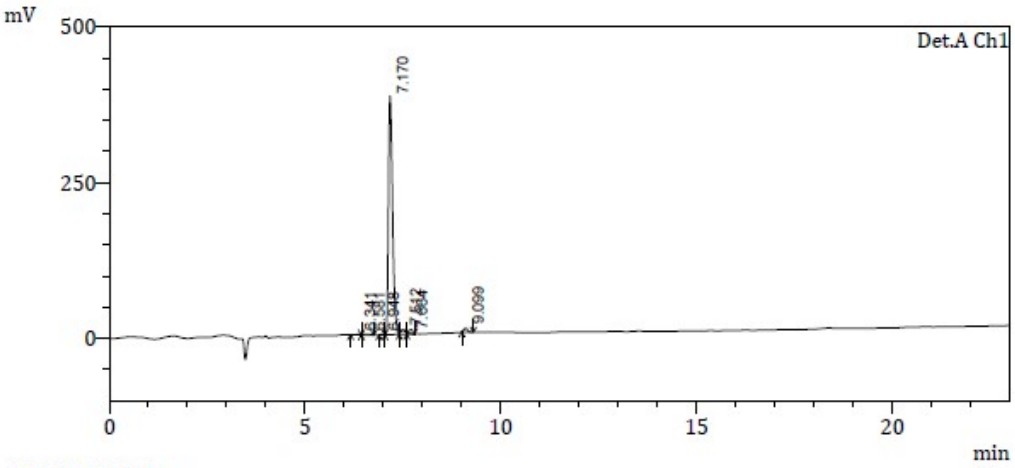

1 Det.A Ch1/220nm

PeakTable

Detector A Ch1 220nm

Peak#	Ret. Time	Area	Height	Area %	Height %
1	6.341	6827	573	0.234	0.143
2	6.581	14632	1152	0.502	0.287
3	6.948	6215	1047	0.213	0.261
4	7.170	2768382	383111	95.039	95.345
5	7.512	61035	6858	2.095	1.707
6	7.664	17595	2942	0.604	0.732
7	9.099	38221	6132	1.312	1.526
Total		2912906	401815	100.000	100.000

Fig. S11 HPLC analysis of the customized probe oligopeptide sequence.

Table S2. Performance correlation of the prepared biosensor against the Ct score of validated clinical sample.

Electrode	Cycle threshold (Ct) score	Current density j(μA/cm^2)
BSA-Pep/b-EgGC	VTM (blank)	0.83
	258	0.69
	255	0.64
	250	0.56
	249	0.54

VTM: viral transport medium. Ct score determined from reverse transcription polymerase chain reaction (RT-PCR) on the selected clinical samples. Current density measured from the chronoamperometry method.

Table S3. Analytical performance of the developed sensor platform with other electrochemical studies.

S. No.	Sensor component / redox system studied on COVID diagnosis	Linear range	Limit of detection	Reference
1.	Dual redox signal provided from horseradish peroxidase substrate with trimethylamine anchoring H_2O_2	1 fM to 100 nM	1 fM	4
2.	Potassium ferri/ferro cyanide as external redox mediator	2.2 to 111 fM	15 fM	5
3.	Methylene blue (MB) and acridine orange (AO) were coated onto silica nanoparticles (SiNPs)	1 to 1×10^9 copies/µL	1 copy/µL	6
4.	Potassium ferri/ferro cyanide as external redox mediator	fg/mL to ng/mL (value not mentioned)	7.2 fg/mL	7
5.	Potassium ferri/ferro cyanide as external redox mediator	Nanomolar range	1.68 ng mL^{-1}	8
6.	Ruthenium hexamine and potassium ferri/ferro cyanide as external redox mediator	1 – 15 µM	0.50 µM	9
7.	Electrochemically grafted GA-CS (*in situ* probe)	100 fg/mL to 1 ng/mL	67.6 fg/mL	This study

References

1. P. Kanagavalli, M. Natchimuthu Karuppusamy, V. S. Ganesan, H. P. Saravanan, T. Palanisamy and M. Veerapandian, *Langmuir*, 2023, **39**, 3512-3525.
2. S. Kumar, A. Patel, L. Lai, C. Chakravarthy, R. Valanparambil, E. S. Reddy, K. Gottimukkala, M. E. Davis-Gardner, V. V. Edara, S. Linderman, K. Nayak, K. Dixit, P. Sharma, P. Bajpai, V. Singh, F. Frank, N. Cheedarla, H. P. Verkerke, A. S. Neish, J. D. Roback, G. Mantus, P. K. Goel, M. Rahi, C. W. Davis, J. Wrammert, S. Godbole, A. R. Henry, D. C. Douek, M. S. Suthar, R. Ahmed, E. Ortlund, A. Sharma, K. Murali-Krishna and A. Chandele, *Science Advances*, 2022, **8**, eadd2032.
3. S. Priya, N. S. Kumar and S. Hemalatha, *Computational Biology and Chemistry*, 2018, **77**, 402-412.
4. Y. Dou, Z. Huang, T. Li, N. Maboyi, X. Ding, S. Song and J. Su, *Chemical Communications*, 2023, **59**, 8838-8841.
5. A. Raziq, A. Kidakova, R. Boroznjak, J. Reut, A. Öpik and V. Syritski, *Biosensors and Bioelectronics*, 2021, **178**, 113029.
6. T. Chaibun, J. Puenpa, T. Ngamdee, N. Boonapatcharoen, P. Athamanolap, A. P. O'Mullane, S. Vongpunsawad, Y. Poovorawan, S. Y. Lee and B. Lertanantawong, *Nature Communications*, 2021, **12**, 802.
7. F. Jiang, Z. Xiao, T. Wang, J. Wang, L. Bie, L. Saleh, K. Frey, L. Zhang and J. Wang, *Chemical Communications*, 2022, **58**, 7285-7288.
8. V. J. Vezza, A. Butterworth, P. Lasserre, E. O. Blair, A. MacDonald, S. Hannah, C. Rinaldi, P. A. Hoskisson, A. C. Ward, A. Longmuir, S. Setford, E. C. W. Farmer, M. E. Murphy and D. K. Corrigan, *Chemical Communications*, 2021, **57**, 3704-3707.
9. N. S. Zambry, M. S. Awang, K. K. Beh, H. H. Hamzah, Y. Bustami, G. A. Obande, M. F. Khalid, M. Ozsoz, A. A. Manaf and I. Aziah, *Lab on a Chip*, 2023, **23**, 1622-1636.